Reliable leak detection in a heat exchanger of a sodium-cooled fast reactor

Blaise Kévin Guépié, Edith Grall-Maës, Pierre Beauseroy, Igor V. Nikiforov, Frédéric Michel

▶ **To cite this version:**

Blaise Kévin Guépié, Edith Grall-Maës, Pierre Beauseroy, Igor V. Nikiforov, Frédéric Michel. Reliable leak detection in a heat exchanger of a sodium-cooled fast reactor. Annals of Nuclear Energy, 2020, 142, pp.107357. 10.1016/j.anucene.2020.107357 . hal-02480730

HAL Id: hal-02480730
https://utt.hal.science/hal-02480730v1

Submitted on 21 Jul 2022

HAL is a multi-disciplinary open access archive for the deposit and dissemination of scientific research documents, whether they are published or not. The documents may come from teaching and research institutions in France or abroad, or from public or private research centers.

L'archive ouverte pluridisciplinaire **HAL**, est destinée au dépôt et à la diffusion de documents scientifiques de niveau recherche, publiés ou non, émanant des établissements d'enseignement et de recherche français ou étrangers, des laboratoires publics ou privés.

Distributed under a Creative Commons Attribution - NonCommercial 4.0 International License

Version of Record: https://www.sciencedirect.com/science/article/pii/S0306454920300554
Manuscript_08287cefdf9eed2d0eaa9938326f8965

Reliable leak detection in a heat exchanger of a sodium-cooled fast reactor☆

Blaise Kevin Guépié, Edith Grall-Maës, Pierre Beauseroy, Igor Nikiforov*

UTT/ICD/LM2S, FRE CNRS, Université de Technologie de Troyes, 12, rue Marie Curie CS 42060 10004 Troyes Cedex, France

Frédéric Michel

CEA, DEN/CAD/DTN/STCP/LISM, Commissariat à l'Energie Atomique et aux Energies Alternatives, Bâtiment 202, 13108 Saint-Paul-lez-Durance, France

Abstract

The heat exchanger (HE) should be permanently monitored in order to detect water or nitrogen leaking into a sodium circuit, which can affect the sodium-cooled fast reactor (SFR) performance or safety. The HE must be shut down in a few seconds after the beginning of the leak, even very small, and repaired. The solution developed in the paper is based on the reliable detection of abrupt changes in the spectral density of measured vibro-acoustic signals. The main difficulty lies in the fact that the small HE leaks have to be detected in the presence of high normal operating noise coming from different equipment (pumps, turbine, etc.). The records from experimental mock-ups dedicated to sodium-gas HE studies and installed at the Commissariat à l'energie atomique et aux energies alternatives (CEA) have been used to assess the proposed solution. The significance of this research with respect to the previous works is twofold. First, the proposed solution detects a small leak in the sodium-gas HE with the signal-to-noise ratio SNR ≥ -30 dB provided that the detection delay is upper bounded by 60 sec, the probability of missed detection is upper bounded by

☆This work has been presented in part at the 18th Annual Conference of the European Network for Business and Industrial Statistics, September 2-6, 2018, Nancy, France. This work has been supported by the Commissariat à l'Energie Atomique et aux Energies Alternatives (CEA), France.

*Corresponding author

© 2020 published by Elsevier. This manuscript is made available under the CC BY NC user license
https://creativecommons.org/licenses/by-nc/4.0/

10^{-5} and the probability of false alarm (per hour) is upper bounded by $10^{-5}\mathrm{h}^{-1}$, which is much better than the usually requested SNR of -17 dB. Second, the analytical formulas for calculation of the probabilities of missed detection and false alarm have been proposed that guarantees the required statistical properties of the proposed test.

Keywords: Sodium-cooled fast reactors, Heat exchanger leak detection, Accelerometer vibro-acoustic signal, Spectral analysis, Periodogram, Finite moving average, Exponential distribution

1. Introduction and motivation

SFRs are used for supplying electricity, utilizing uranium resources better and reducing the total radiotoxicity of nuclear waste, in comparison with the commonly used light water nuclear reactors. The SFRs have to transfer energy from the secondary to the tertiary circuit. In a sodium-water HE, if a leak occurs, the water comes into contact with the sodium and generates a violent exothermic reaction which quickly compromises the integrity of the affected secondary circuit. Hence, leak detection is a crucially important task for ensuring the safety of SFRs. In [1], the leak detection is achieved by using a chemical hydrogen detection system. Unfortunately, the detection time is rather long. In order to realize long-time monitoring with a shorter response during the HE leakage, the signal processing of accelerometer vibro-acoustic signals and different statistical detection methods are discussed in [2, Ch. 10–13]. The prediction of loss of coolant activity (LOCA) in a different but similar framework based on the vibro-acoustic signal spectral analysis is proposed in [3]. The prediction of the leak rate in the framework of the leak before break (LBB) concept by genetic neural network and genetic algorithms are studied in [4]. An experimental small leak of steam into the sodium loop is considered in [5, 6]. According to these papers, a leak in the HE leads to a change of the accelerometer vibro-acoustic signal power spectral density (PSD). A leak detection algorithm based on the hidden Markov model (HMM) and the Gaussian mixture model (GMM)

of the representation of the vibro-acoustic signal has been proposed. Because the vibrations induced by a leak of steam into the sodium loop can be masked by background noise, the increasing of the SNR by switching from a single sensor to an array of sensors is an important and promising task. Another limitation of a single vibro-acoustic sensor is the difficulty to estimate the leak position/orientation/flow rate by using a single sensor. In fact, the leak sound intensity and/or the spectrum of vibro-acoustic signal cannot be directly linked to the leak position/orientation/flow rate (see, for instance, [7]). The techniques of beam forming and phased array applied to the outputs of the vibro-acoustic sensor array to increase the SNR has been studied in [8, 9] and to separate the acoustic source from background noises in [10]. Another advantage of the sensor array for improving the sodium-water HE safety is the estimation of the leak position (see details in [8, 10]).

In order to avoid/minimize the risk of damage of the HE, a new type of HE is currently studied by the CEA through the ASTRID [1] project [11]. This new HE includes the use of the sodium-gas pair (sodium-nitrogen). Even if there is no risk of an exothermic chemical reaction using a sodium-nitrogen HE, a leak of nitrogen into the sodium circuit will affect the reactor performance and have to be reliably detected during 60 sec after a small leak appearance. It is considered that if the leak is not detected within the first 60 sec it can lead to a degradation of the HE or SFR performance. The leak detection task remains difficult due to the presence of high normal operating noise coming from the process (water boiling, turbulence, etc.), different equipment (pumps, turbine, etc.) and due to the change of the reactor operating mode. This problem remains largely unresolved. The only recent paper [12] devoted to this problem considers the algorithm based on the HMM and GMM of the vibro-acoustic signals coupled with the cumulative sum (CUSUM) algorithm and used as a monitoring method for the sodium-gas HE. Unfortunately, none of the previously mentioned papers investigate any analytical expression relating to

[1] ASTRID means the advanced sodium technological reactor for industrial demonstration.

the detection delay, the false alarm rate, and the missed detection probability, which are crucially important for monitoring safety-critical systems required for the SFR HE. This problem is especially significant because the conventional Monte Carlo statistical simulation of detection algorithms is not efficient due to the very small target values of the probabilities of false alarm and missed detection.

The statistical theory adapted to safety-critical system monitoring has recently been developed for the reliable detection of abrupt changes in random signals (see [13, 14, 15, 16]). The goal of this paper is to adapt this statistical theory to the HE leak detection problem. Despite the fact that the current paper is devoted to the detection of leaks in sodium-nitrogen HEs, the obtained results can be considered as the first step towards achieving a method of online vibro-acoustic monitoring for a more general class of HE and other equipment.

To assess the performance of the SFR HE leak detection algorithm, the experiments are often built to be more or less representative of a real leak. It is done by water, hydrogen or neutral gas injection through the side wall of a real full scale or reduced HE [17, 18] or in another representative loop [19, 8]. To be able to test the method with various SNR values, either the pressure can be decreased, often leading to a non-representative pressure, or the signal can be numerically mixed with background noise [21, 22].

The original contribution of this paper is threefold.

- The problem of HE leak detection is reduced to the reliable sequential detection of changes in the spectrum of vibro-acoustic signals. The finite moving average (FMA) test has been redesigned from the time domain to the frequency domain.
- The asymptotic equations for the probabilities of false alarm and missed detection have been proposed to quantitatively predict the statistical properties of the FMA test in the frequency domain.
- The assessment of the proposed test has been carried out by using the mix of records of normal operating noise and the records of abnormal

noise (due to small leaks) from experimental mock-ups installed at the CEA and obtained in the framework of the ASTRID project.

This paper is organized as follows. Section 2 states the problem of the HE leak detection. Section 3 is devoted to the proposed solution. Here we briefly present the theoretical background, the design of the leak detection algorithm and its asymptotic statistical properties. Section 4 describes the experimental data and Section 5 uses the proposed algorithm and presents the results of simulation and data processing. Some extensions of the proposed leak detection algorithm are discussed in Section 6. Finally, conclusions are drawn in Section 7.

2. Problem statement

The leak detection system uses accelerometers equipped with an analog-to-digital converter, which converts continuous-time analog signals to discrete-time digital signals. Let us define the discrete time vibro-acoustic signal $\{y_n\}_{n\geq 0}$. The generative model of this signal is given by the following equation

$$y_n = \begin{cases} x_n & \text{if} \quad n < t_0, \\ x_n + s_n & \text{if} \quad n \geq t_0, \end{cases} \tag{1}$$

where $\{x_n\}_{n\geq 0}$ is the vibro-acoustic signal corresponding to normal operating noise coming from the HE and from other equipment (pumps, turbine, etc.), $\{s_n\}_{n\geq t_0}$ is the vibro-acoustic signal corresponding to a small leak in the HE and t_0 is the unknown "change-point" (in the context of leak detection, t_0 is the instant of a leak appearance). In contrast to the Bayesian approach, no *a priori* information is available on the distribution of t_0 in the context of leak detection. For this reason the unknown "change-point" t_0 is assumed to be non-random.

Following the preliminary experimental study, the distributions of the vibro-acoustic signals $\{x_n\}_{n\geq 0}$ and $\{s_n\}_{n\geq t_0}$ can be approximated by a zero-mean Gaussian law. The variances of $\{x_n\}_{n\geq 0}$ and $\{s_n\}_{n\geq t_0}$ vary due to different normal operating and leak conditions. The only distinguishable feature for the detection of $\{s_n\}_{n\geq t_0}$ is the shape of the signal PSD at a certain interval of

frequencies. To decide between the hypotheses $\{\mathcal{H}_0 : y_n = x_n\}$ (normal operating noise coming from different equipment) and $\{\mathcal{H}_1 : y_n = x_n + s_n\}$ (normal operating noise plus the signal corresponding to a leak), we need to estimate the PSD, which represents the distribution of signal energy as a function of frequency. Two different methods of spectral analysis have been used : the periodogram (by using the fast Fourier transform (FFT)) and the autoregressive (AR) model [23, 24, 25, 26, 27].

The periodogram is calculated by using the Bartlett-Welch method by averaging multiple periodograms. The record $(y_0, \ldots, y_{N-1})$ is subdivided into K smaller disjoint segments of size L, where L is an even number, i.e., $N = KL$. The periodogram is calculated for the set of frequencies $f_k = \dfrac{k}{L} F_s$, $k = 0, 1, 2, \ldots, \dfrac{L}{2}$ by using the

$$\widehat{S}_y(f_k) = \frac{1}{K} \sum_{i=0}^{K-1} \widehat{S}_y^i(f_k), \quad \widehat{S}_y^i(f_k) = \frac{1}{F_s L} \left| \sum_{n=0}^{L-1} h_n y_{n+iL} e^{-jn\frac{2\pi k}{L}} \right|^2, \qquad (2)$$

where j is the imaginary number, $j^2 = -1$, f_k is the frequency measured in hertz (Hz), F_s is the sampling frequency measured in Hz, $h_0, \ldots, h_{L-1}$ is a normalized window function. The periodogram is a consistent estimate of the PSD provided that $K \to \infty$ and $L \to \infty$. The second method of spectral analysis is based on the parametric approach. It is assumed that the observations $\{y_n\}_{n \geq 0}$ are generated by the following AR(p) model of order p :

$$y_n = \sum_{i=1}^{p} \alpha_i y_{n-i} + \xi_n, \quad \xi_n \sim \mathcal{N}(0, \sigma_\xi^2), \qquad (3)$$

where $\mathcal{N}(0, \sigma_\xi^2)$ denotes a zero-mean Gaussian distribution with variance σ_ξ^2. The parametric AR(p) estimation of the PSD is therefore given by

$$\widehat{S}_y(f) = \frac{2\widehat{\sigma}_\xi^2}{F_s \left| 1 - \sum_{i=1}^{p} \widehat{\alpha}_i e^{-j\frac{2\pi f i}{F_s}} \right|^2}, \quad 0 \leq f \leq \frac{F_s}{2}, \qquad (4)$$

where the estimations $\widehat{\alpha}_i$ of the AR coefficients α_i, $i = 1, \ldots, p$ and variance $\widehat{\sigma}_\xi^2$ are obtained by the resolution of maximum likelihood equations (either Yule-Walker equations or by other methods) [23, 26, 27]. If the order p is correctly defined then the estimation of the PSD is consistent.

To detect a leak in the HEs, one has to design a detector which is sensitive to the changes in the PSD related to the leak and, simultaneously, insensitive to the changes of the normal operating mode. The PSD function $f \mapsto S_y(f)$ contains useful information (an informative parameter) related to the leak only at a certain interval, for $f \in [f_1, f_2]$, where $0 < f_1 < f_2 < F_s/2$. The PSD at all other frequencies $f \notin [f_1, f_2]$ is considered as a nuisance parameter and its negative impact on the detector should be minimized. In such a situation, the usage of parametric models like AR (or even autoregressive - moving average (ARMA)) appears to be limited. Indeed, the shape of the parametric-based PSD $f \mapsto S_y(f)$ at the interval $[0, F_s/2]$ is defined by all the parameters of AR or ARMA model. It is tricky to find a subset of AR parameters $\alpha_1, \ldots, \alpha_p$ which defines a prescribed shape for $f \in [f_1, f_2]$ and, which is simultaneously independent of the parametric-based PSD at other frequencies $f \notin [f_1, f_2]$. Moreover, the covariance matrix of the AR vector is non-diagonal. This fact also leads to additional problems in the separation of informative and nuisance parameters.

On the contrary, the periodogram $\widehat{S}_y(f_k)$ calculated at a set of frequencies $f_k = \dfrac{k}{L}F_s$, $k = 0, 1, 2, \ldots, L/2$ represents a non-parametric model of the spectrum. Such a model is more flexible because $\widehat{S}_y(f_k)$ and $\widehat{S}_y(f_\ell)$, estimated at different frequencies f_k and f_ℓ with $k \neq \ell$, are asymptotically independent when $L \to \infty$ [24, 25, 26, 27]. This justifies the statistical exclusion of a nuisance parameter. A set of frequencies f_k, where $k \in \{k_1, \ldots, k_2\}$ and $0 \leq k_1 \leq k_2 \leq L/2$, is used to design a leak detector. The PSD at all other frequencies f_k such that $k \notin \{k_1, \ldots, k_2\}$ is considered as an independent nuisance parameter and, hence, excluded from the consideration. Finally, the leak detection based on the PSD can be easily suitable to increase the SNR by using the technique of beam forming, see, for instance, [8, 9, 28].

Therefore, as of now it is assumed that the discrete time vibro-acoustic signal $\{y_n\}_{n\geq 0}$ is sequentially subdivided into segments of size L, where L is an even number. The sequence of segments $\{Y_i\}_{i\geq 1}$ is considered. The i th segment is defined as $Y_i = (y_{(i-1)L}, \ldots, y_{iL-1})$. Let us rewrite the generative model of

observations given by (1). First of all :

$$S_y^i(f) = \begin{cases} S_x(f) & \text{if} \quad i < i_0, \\ S_{x+s}(f) & \text{if} \quad i \geq i_0 \end{cases} \quad \text{for} \;\; f \in [f_1, f_2], \tag{5}$$

where i_0 is the change-point expressed in number of segments, $S_y^i(f)$ is the PSD of the i th segment Y_i, $S_x(f)$ is the PSD of normal operating noise and $S_{x+s}(f)$ is the PSD of the additive sum of normal operating noise and the signal due to a leak. It follows from [24, 25, 26, 27] that asymptotically

$$\widehat{S}_y^i(f_k) \sim \text{Exp}\left(S_y^i(f_k)\right) \;\; \text{for} \;\; f_k = \frac{k}{L} F_s \;\; \text{and} \;\; k = 0, 1, 2, \ldots, \frac{L}{2}, \tag{6}$$

where $\widehat{S}_y^i(f_k)$ is the periodogram calculated for the i th segment Y_i and $\text{Exp}(\mu)$ is an exponential distribution with mean μ. Finally, the generative model of segments is given by

$$\widehat{S}_y^i(f_k) \sim \begin{cases} \text{Exp}\left(S_x(f_k)\right) & \text{if} \quad i < i_0, \\ \text{Exp}\left(S_{x+s}(f_k)\right) & \text{if} \quad i \geq i_0 \end{cases} \quad \text{for} \;\; f_k = \frac{k}{L} F_s \;\; \text{and} \;\; k = k_1, \ldots, k_2, \tag{7}$$

where $0 \leq k_1 \leq k_2 \leq L/2$. Obviously, the subdivision of the initial sequence $\{y_n\}_{n \geq 0}$ into the sequence of segments induces an additional detection delay which is upper bounded by L. In the current study $F_s = 51.2$ kilohertz (kHz) and $L = 8192$, then the duration of one segment is 0.16 sec and the worst case additional delay caused by the segmentation is equal to 0.16 sec, which is negligible with respect to (w.r.t.) the required time-to-alert of 60 sec. Therefore, the HE leak detection is reduced to the sequential detection of abrupt changes in the distribution of the vector of peridodogram $\left(\widehat{S}_y^i(f_{k_1}) \ldots, \widehat{S}_y^i(f_{k_2})\right)$ of the observed sequence of segments.

3. Proposed solution : reliable detection of abrupt changes

3.1. Sequential detection of abrupt changes

The goal of this section is to briefly introduce the sequential detection of abrupt changes in random signals [29, 30, 31, 32]. We begin with the classical

optimality criterion, which involves the minimization of the (worst-case) mean detection delay provided that a prescribed level of false alarms is satisfied. The Bayesian approach to this problem and its optimal solution have been proposed by Shiryaev [33, 34]. Let us consider the non-Bayesian framework, where the "change-point" t_0 is unknown but non-random. Let $\{y_n\}_{n\geq 1}$ be the sequence of independent random variables and let t_0 be the index of the first post-change observation:

$$y_n \sim \begin{cases} F_0 & \text{if} \quad n < t_0, \\ F_1 & \text{if} \quad n \geq t_0, \end{cases} \tag{8}$$

where F_0 is the pre-change cumulative distribution function (CDF) and F_1 is the post-change CDF. Let $\mathcal{P}_{t_0}$ be the joint distribution of the observations $y_1, y_2, \cdots, y_{t_0}, y_{t_0+1}, \cdots$ when $t_0 < \infty$. Let $\mathcal{P}_0$ denote the same when $t_0 = \infty$, i.e., there is no change and all the observations $y_1, y_2, \cdots$ are i.i.d. with CDF F_0. Let $\mathbb{E}_{t_0}$ (resp. $\mathbb{E}_0$) and $\mathbb{P}_{t_0}$ (resp. $\mathbb{P}_0$) be the expectation and probability w.r.t. the distribution $\mathcal{P}_{t_0}$ (resp. $\mathcal{P}_0$). Lorden [35] proposed an optimality criterion, which involves the minimization of the worst-case mean detection delay:

$$\inf_{T\in C_\eta} \left\{ \overline{\mathbb{E}}(T) \stackrel{\text{def}}{=} \sup_{t_0\geq 1} \operatorname{esssup} \mathbb{E}_{t_0}\Big[(T-t_0+1)^+ \,|y_1, \ldots, y_{t_0-1}\Big] \right\}, \quad (x)^+ \stackrel{\text{def}}{=} \max(0,x), \tag{9}$$

where $T \in \{1, 2, \ldots\}$ is a stopping time w.r.t. the sequence of random variables $\{y_n\}_{n\geq 1}$, i.e., an integer random variable such that, for every $n \geq 1$, the event $\{T = n\}$ depends only on the variables $y_1, y_2, ..., y_n$, among all stopping times T belonging to the class

$$C_\eta = \{T : \mathbb{E}_0(T) \geq \eta\}, \tag{10}$$

where $\eta > 0$ is a prescribed value of the average run length (ARL) to a false alarm. Lorden proved that the CUSUM test, previously introduced by Page [36], is asymptotically optimal w.r.t. criterion (9) – (10). A non asymptotic optimality of the CUSUM test has been established by Moustakides [37]. The stopping time (the time of decision) T_{CS} of the CUSUM test is given by

$$T_{\text{CS}} = \inf \left\{ n \geq 1 : \max_{1\leq k\leq n} \sum_{i=k}^{n} \log \frac{p_1(y_i)}{p_0(y_i)} \geq h \right\}, \tag{11}$$

where p_0 denotes the pre-change probability density function (PDF), p_1 denotes the post-change PDF and h is the threshold. Recent results on the application of the CUSUM test to more general statistical models (ARMA model,...) can be found in [38, 39, 40, 32].

The traditional criterion, like (9) – (10), which involves the minimization of the (worst-case) mean detection delay provided that the ARL to a false alarm is lower bounded by a given constant, is based on the idea initially proposed by Wald [41]. This idea is motivated by the economic criterion in quality control when the price of each new observation is constant. Using criterion (9) – (10), we accept that some run lengths will be very long, some other – very short, but, in the *mean*, the detection delay will be acceptable. Unfortunately, the criterion (9) – (10) is unacceptable for safety-critical applications. The price of each new observation depends on the detection delay in safety-critical applications. If the delay for detection is greater than the required time-to-alert N, the price of each new observation is infinitely higher than the price of observation if the delay for detection is less than or equal to N. For this reason, we propose using another criterion of reliable detection, which involves the minimization of the worst-case probability of missed detection provided that the worst-case probability of false alarm per a given reference period m_α is upper bounded [13, 14, 15, 16].

The reliable detection of (transient) changes is motivated by two possible scenarios. The first scenario corresponds to the situation when the observed phenomena (say, underwater acoustic signal) is of short and maybe unknown (and random) duration Γ. It is called a transient change detection problem [42, 43, 44, 45, 46, 47]. Sometimes even the "latent" detection (i.e., the detection after the end of transient change) is acceptable. The second scenario arises when the observed anomaly (navigation equipment fault, leak in the HE,...) leads to serious degradation of the system security when the change is detected with the delay greater than the required time-to-alert N, i.e., $T - t_0 + 1 > N$. It is called a reliable detection of (transient) changes. In the framework of this second scenario, the duration Γ of the transient change is assumed to be sufficient, at least $\Gamma \geq N$. If the transient change is detected with the detection delay greater

than N, it is assumed to be missed [13, 14, 15, 16]. On the other hand, if the true duration Γ of the transient change is smaller than the required time-to-alert N, i.e., $\Gamma < N$ then such a transient change is considered as less dangerous because its impact on the system is limited or negligible.

Let us formalize the reliable detection problem. We consider the sequence of random variables $\{y_n\}_{n\geq 1}$. Let t_0 be the index of the first post-change observation (unknown and non random). The latest but still acceptable detection happens when the stopping time is $T = n = t_0 + N - 1$. It doesn't matter what happens after the instant $n = t_0 + N - 1$, the transient change is missed. For this reason the duration of the transient change (post-change period) is assumed to be $\Gamma = N$:

$$y_n \sim \begin{cases} F_0 & \text{if} \quad 1 \leq n < t_0 \\ F_1 & \text{if} \quad t_0 \leq n \leq t_0 + N - 1 \end{cases} \tag{12}$$

where F_0 is the pre-change CDF and F_1 is the post-change CDF during the transient change period. As previously, it is assumed that $\mathcal{P}_{t_0}$ is the joint distribution of the observations $y_1, \cdots, y_{t_0}, y_{t_0+1}, \cdots$ when $t_0 < \infty$. Because the considered subclass of stopping times is based on the variable-threshold truncated sequential probability ratio tests (SPRT), the existence of a short "pre-heating" period N is assumed. This short period is necessary to accumulate the first N observations $y_1, y_2, ..., y_N$ in order to avoid the situation where the truncated SPRT performs by using an insufficient number of observations. The quality of a statistical decision cannot be guaranteed if the number of observations is less than the required time-to-alert N. Finally, the optimality criterion used in this paper is given by [14, 15, 16]. It involves the minimization of the worst-case probability of missed detection $\overline{\mathbb{P}}_{\mathrm{md}}(T)$:

$$\inf_{T \in C_\alpha} \left\{ \overline{\mathbb{P}}_{\mathrm{md}}(T) \stackrel{\mathrm{def}}{=} \sup_{t_0 \geq N} \mathbb{P}_{t_0}(T - t_0 + 1 > N \mid T \geq t_0) \right\}, \tag{13}$$

among all stopping times $T \in C_\alpha$ satisfying

$$C_\alpha = \left\{ T : \overline{\mathbb{P}}_{\mathrm{fa}}(T; m_\alpha) \stackrel{\mathrm{def}}{=} \sup_{\ell \geq N} \mathbb{P}_0(\ell \leq T < \ell + m_\alpha) \leq \alpha \right\}, \tag{14}$$

where $\overline{\mathbb{P}}_{\mathrm{fa}}(T; m_\alpha)$ is the worst-case probability of false alarm during the reference period m_α measured in discrete time.

The design of the transient change detector is discussed in [14, 15, 16]. Let us briefly define the FMA test obtained from a more general variable threshold window limited (VTWL) CUSUM test. As it follows from [16, Theorem 3], the optimization of the VTWL CUSUM test in a subclass of truncated SPRT leads to the FMA test. The stopping time T_{FMA} of the FMA test is given as follows

$$T_{\mathrm{FMA}} = \inf\left\{n \geq N : \Lambda_{n-N+1}^{n} \geq h\right\}, \;\; \Lambda_{n-N+1}^{n} = \sum_{i=n-N+1}^{n} \log \frac{p_1(y_i)}{p_0(y_i)}, \quad (15)$$

where Λ_{n-N+1}^{n} is the log-likelihood ratio (LLR). To get the upper bounds for the probabilities $\overline{\mathbb{P}}_{\mathrm{md}}(T_{\mathrm{FMA}})$ (13) and $\overline{\mathbb{P}}_{\mathrm{fa}}(T_{\mathrm{FMA}}; m_\alpha)$ (14), it is necessary to meet some technical conditions and define several probabilities and their bounds. The details can be found in [15, 16]. Following [16, Theorem 1], the worst-case probability of missed detection $\overline{\mathbb{P}}_{\mathrm{md}}(T_{\mathrm{FMA}})$ is upper bounded as follows

$$\overline{\mathbb{P}}_{\mathrm{md}}(T_{\mathrm{FMA}}) \leq G(h) \stackrel{\mathrm{def}}{=} \mathbb{P}_{t_0}\left(\Lambda_{t_0}^{N+t_0-1} < h\right), \; t_0 \geq N, \quad (16)$$

where $\mathbb{P}_{t_0}\left(\Lambda_{t_0}^{N+t_0-1} < h\right)$ corresponds to the probability of missed detection of the Neyman-Pearson LLR test calculated for the time window $[t_0, t_0 + N - 1]$ and the threshold h.

Let us assume that the CDF of the LLR Λ_{n-N+1}^{n}

$$x \mapsto F(x) \stackrel{\mathrm{def}}{=} \mathbb{P}_0\left(\Lambda_{n-N+1}^{n} \leq x\right) \quad (17)$$

is a continuous function on $]-\infty; \infty[$ under the measure $\mathcal{P}_0$ and that the LLRs are associated under the probability measure $\mathcal{P}_0$ [16, Theorems 2 and 3]. Following [16, Theorems 2 and 3], the worst-case probability of false alarm $\overline{\mathbb{P}}_{\mathrm{fa}}(T_{\mathrm{FMA}}; m_\alpha)$ for a given pre-changed period m_α is upper bounded by

$$\overline{\mathbb{P}}_{\mathrm{fa}}(T_{\mathrm{FMA}}; m_\alpha) \leq H(h) \stackrel{\mathrm{def}}{=} 1 - [F(h)]^{m_\alpha}. \quad (18)$$

Provided that the upper bound for the worst-case probability of false alarm $H(h)$ is equal to a pre-assigned value $\overline{\alpha}_0$, the smallest value $\overline{\alpha}_1$ of the upper bound $G(h)$ is given by [15, 16]

$$\overline{\alpha}_1 = G\left[F^{-1}\left((1-\overline{\alpha}_0)^{\frac{1}{m_\alpha}}\right)\right]. \quad (19)$$

Finally, the optimal threshold is given by [15, 16]

$$h = F^{-1}\left((1-\overline{\alpha}_0)^{\frac{1}{m_\alpha}}\right). \tag{20}$$

3.2. Sequential detection of spectral changes

The generative model of vibro-acoustic signals with an abrupt change has been defined in (1), (5) and (7). This model describes the spectral changes of the observed signal $\{y_n\}_{n\geq 0}$ related to the HE leaks. It follows from (7) that the null and alternative hypotheses are defined for each segment i of size L and for each frequency f_k as :

$$\mathcal{H}_0 \ : \widehat{S}_y^i(f_k) \sim \mathrm{Exp}\left(S_x(f_k)\right) \text{ against } \mathcal{H}_1 \ : \widehat{S}_y^i(f_k) \sim \mathrm{Exp}\left(S_{x+s}(f_k)\right) \tag{21}$$

where $f_k = F_s k/L$, $k \in \{k_1, \ldots, k_2\}$, $0 \leq k_1 \leq k_2 \leq \frac{L}{2}$. Let us rewrite the LLR (15) by taking into account the asymptotic assumptions that the estimations $\widehat{S}_y^i(f_k)$ and $\widehat{S}_y^i(f_\ell)$, $k \neq \ell$, are independent and the estimations $\widehat{S}_y^i(f_k)$ and $\widehat{S}_y^j(f_k)$ calculated by using the i-th and j-th segments of size L, $i \neq j$, are asymptotically uncorrelated when $K \to \infty$ and $L \to \infty$ [23, 24, 25, 26, 27]. Following the definition of the exponential law $\mathrm{Exp}(\mu)$, its PDF is given by

$$p_\mu(x) = \begin{cases} \frac{1}{\mu} e^{-\frac{x}{\mu}} & \text{if} \quad x \geq 0, \\ 0 & \text{if} \quad x < 0, \end{cases} \tag{22}$$

where μ is mean. The LLR between the hypotheses $\mathcal{H}_0$ and $\mathcal{H}_1$ for the frequency f_k and for the record $(y_0, \ldots, y_{N-1})$ subdivided into K segments of size L, i.e., $N = KL$, is written as follows

$$\Lambda_1^K(f_k) = \sum_{i=1}^{K} \Lambda_i(f_k), \quad \Lambda_i(f_k) = \log \frac{S_x(f_k)}{S_{x+s}(f_k)} + \left[\frac{1}{S_x(f_k)} - \frac{1}{S_{x+s}(f_k)}\right] \widehat{S}_y^i(f_k), \tag{23}$$

where i is the number of a segment of size L, $i = 1, 2 \ldots, K$, $\widehat{S}_y^i(f_k)$ is the periodogram corresponding to the frequency f_k and calculated for the i-th segment of the record $(y_0, \ldots, y_{N-1})$.

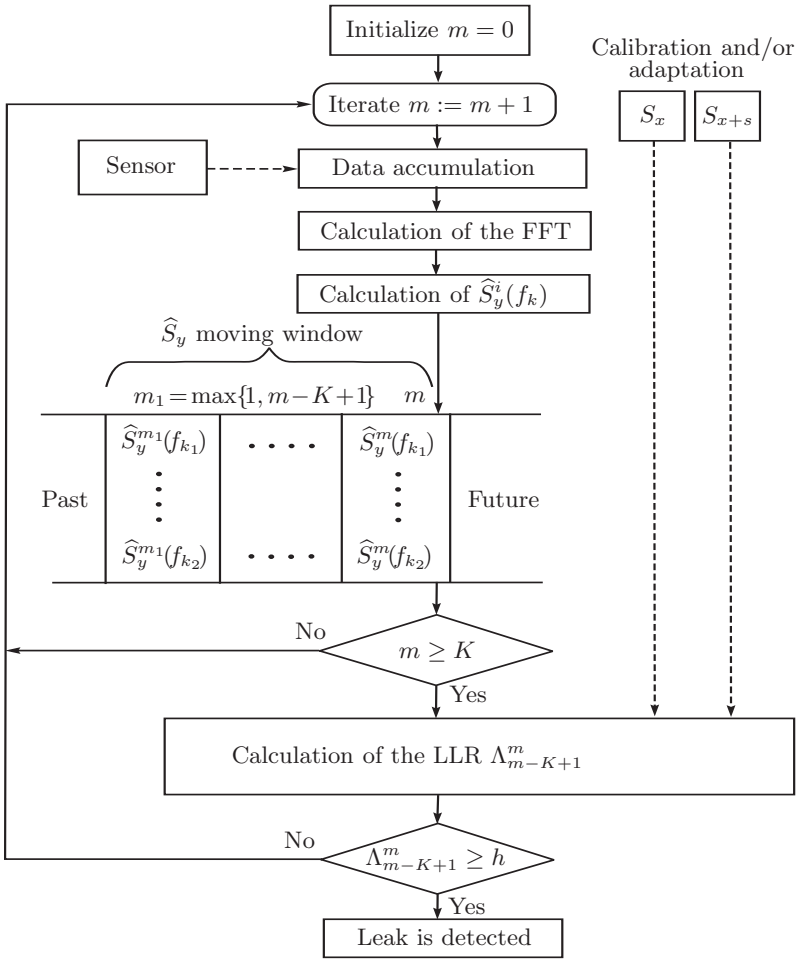

Figure 1: The flowchart of the leak detection algorithm. The flowlines show the process's order of operation and the dashed lines with arrowheads show the transmission of information.

Therefore, the total LLR is obtained by summing the LLR $\Lambda_1^K(f_k)$ (23) over the set of all frequencies $f_{k_1}, \ldots, f_{k_2}$ under consideration

$$\Lambda_1^K = K \sum_{k=k_1}^{k_2} \log \frac{S_x(f_k)}{S_{x+s}(f_k)} + \sum_{k=k_1}^{k_2} \left[\frac{1}{S_x(f_k)} - \frac{1}{S_{x+s}(f_k)} \right] \sum_{i=1}^{K} \widehat{S}_y^i(f_k). \qquad (24)$$

Finally, let us adapt the stopping time T_{FMA} (15) of the FMA test to the detection of spectral changes. Now, the LLR (24) is calculated for the moving

window of vibro-acoustic signal $(y_{mL-KL}, \ldots, y_{mL-1})$ of size $N = KL$, where $m = K, K+1, K+2, \ldots$. This moving window is subdivided into K segments. Hence, the stopping time (i.e., the decision time) is a multiple of L and it is natural to re-write the LLR and stopping rule (15) as a function of the current number m of a segment of size L :

$$T_{\mathrm{FMA}} = \inf\left\{m \geq K : \Lambda_{m-K+1}^{m} \geq h\right\}. \tag{25}$$

The flowchart of the leak detection algorithm is shown in Figure 1. The algorithm is represented by an iterative loop with a stopping condition (realizing the stopping rule defined in (25)). The variable of the loop m denotes the number of the current vibro-acoustic signal segment. The FFT is applied to the m-th segment of the record at each step m. The last $m - m_1 + 1$ periodograms $\widehat{S}_y^{m_1}, \ldots, \widehat{S}_y^{m}$ are stored in a data buffer of maximum size K (see Figure 1). Next, the LLR Λ_{m-K+1}^{m} is calculated for $m \geq K$. This iterative loop is stopped when the condition $\left\{\Lambda_{m-K+1}^{m} \geq h\right\}$ is true for the first time.

3.3. Asymptotic properties of the finite moving average detector

Following equations (16) – (20), to compute the relation between the probabilities $\overline{\alpha}_0$, $\overline{\alpha}_1$ and the threshold h, it is necessary to know the distributions F and G. The total LLR Λ_{m-K+1}^{m} represents a double weighted sum of exponential random variables $\mathrm{Exp}(\mu_{k,i})$ with different means $\mu_{k,i}$. Hence, Λ_{m-K+1}^{m} is distributed following a hypoexponential distribution (or a generalized Erlang distribution) under the hypotheses $\mathcal{H}_0$ and $\mathcal{H}_1$. It can be approximated by a Gaussian distribution for large K and L with negligible approximation errors. Such asymptotic Gaussian approximations for the CDF functions F and G are used in this paper for rough calculation of $\overline{\alpha}_0$, $\overline{\alpha}_1$ and h.

Putting equation (24) together with the expectation $S_y(f_k)$ and variance $S_y^2(f_k)$ of the exponential law $\mathrm{Exp}\left(S_y(f_k)\right)$, we get the expectation and variance of the total LLR

$$\mathbb{E}_S[\Lambda_1^K] = K \sum_{k=k_1}^{k_2} \log \frac{S_x(f_k)}{S_{x+s}(f_k)} + K \sum_{k=k_1}^{k_2} \left[\frac{1}{S_x(f_k)} - \frac{1}{S_{x+s}(f_k)}\right] S_y(f_k). \tag{26}$$

and

$$\mathrm{var}_S[\Lambda_1^K] = K \sum_{k=k_1}^{k_2} \left[\frac{1}{S_x(f_k)} - \frac{1}{S_{x+s}(f_k)} \right]^2 S_y^2(f_k) \tag{27}$$

provided that the true PSD is given by $f \mapsto S_y(f)$. If the hypothesis $\mathcal{H}_0$ is true, then $S_y(f) = S_x(f)$. If the hypothesis $\mathcal{H}_1$ is true, then $S_y(f) = S_{x+s}(f)$. Specifically, let us denote by μ_0 (resp. μ_1) the expectation of the total LLR $\mathbb{E}_S[\Lambda_1^K]$ under hypothesis $\mathcal{H}_0$ (resp. $\mathcal{H}_1$). We also denote by σ_0^2 (resp. σ_1^2) the variance $\mathrm{var}_S[\Lambda_1^K]$ of the total LLR under hypothesis $\mathcal{H}_0$ (resp. $\mathcal{H}_1$). It follows from equations (16) – (20) that

$$\overline{\alpha}_1 = \Phi_{\mu_1,\sigma_1^2} \left[\Phi^{-1}_{\mu_0,\sigma_0^2} \left((1-\overline{\alpha}_0)^{\frac{1}{m_\alpha}} \right) \right], \tag{28}$$

where $x \mapsto \Phi_{\mu,\sigma^2}(x)$ is the CDF of the Gaussian distribution $\mathcal{N}(\mu,\sigma^2)$. Finally, the optimal threshold is given by

$$h = \Phi^{-1}_{\mu_0,\sigma_0^2} \left((1-\overline{\alpha}_0)^{\frac{1}{m_\alpha}} \right). \tag{29}$$

It is worth noting that the required number of segments to alert K and the reference period m_α, used in equations (26) – (29), are measured in number of segments of size L per the required time-to-alert and per reference period measured in sec. Let us assume that the sampling frequency is $F_s = 51.2$ kHz and the segment size is $L = 8192$. For example, if the required time-to-alert is 60 sec and the reference period for false alarm is 3600 sec then the required number of segments to alert is $K = 375$ and the reference period for false alarm measured in number of segments is $m_\alpha = 22500$.

It is also worth noting that the impact of a transient segment of size L which is composed of pre-change and post-change periodograms is assumed to be negligible as it has been shown in Section 2. In the case when this impact is not negligible, the developed theory [16, Theorems 1, 2 and 3] allows to easily adopt the LLR Λ_{m-K+1}^m to the presence of such a transient segment (see also Section 6 for further discussion).

4. Experimental data

The experimental data used in this study come from two different installations at CEA/Cadarache : IKHAR and DIADEMO. The IKHAR experimental installation at CEA/Cadarache is designed to obtain the vibro-acoustic signals corresponding to the nitrogen injection (simulation of a leak) under different pressure in a HE channel. The IKHAR installation uses water instead of sodium for several practical reasons (safety, simplicity, efficiency, etc.). As the leak jet pushes away the liquid outer the concerned channel the obtained noise of nitrogen jet in the nitrogen filled channel is representative (except for temperature). This experiment is further described in [20]. The records coming from this experiment also include the background noise corresponding to water flow without leakage than can be used as a generic background noise. But these signals do not contain normal operating noise coming from a sodium-gas HE and from other equipment (pumps, turbine, etc.) For this reason, the data from another installation, i.e., the DIADEMO sodium loop at CEA/Cadarache, have been used in order to get a condition representative to a real-life nominal operating noise. In the DIADEMO loop, the accelerometer is placed on a flange outside of the sodium-gas HE. At this position, the accelerometer was at a distance of about 0.5 m from the HE but mechanically coupled to it.

In this study, it has been assumed that the null hypothesis $\mathcal{H}_0$ (no leak) is defined as a weighted sum of two vibro-acoustic signals coming from the installations IKHAR and DIADEMO

$$\begin{aligned} \mathcal{H}_0 \ : (y_0, \ldots, y_{N-1}) &= (x_0, \ldots, x_{N-1}) \\ &= \frac{w_1}{\sigma_{x,1}} (x_{0,1}, \ldots, x_{N-1,1}) + \frac{w_2}{\sigma_{x,2}} (x_{0,2}, \ldots, x_{N-1,2}) , \end{aligned} \quad (30)$$

where $x_0, \ldots, x_{N-1}$ is the vibro-acoustic signal corresponding to $\mathcal{H}_0$, $x_{0,1}, \ldots, x_{N-1,1}$ is the vibro-acoustic signal coming from the installation IKHAR corresponding to background noise of water flow without leakage, $x_{0,2}, \ldots, x_{N-1,2}$ is the vibro-acoustic signal coming from the installation DIADEMO, w_1 and w_2 are weighted coefficients of vibro-acoustic signals, $w_1^2 +$

$w_2^2 = 1$, $\sigma_{x,1}$ is the standard deviation (SD) of the signal $\{x_{n,1}\}_{n\geq 0}$ and $\sigma_{x,2}$ is the SD of the signal $\{x_{n,2}\}_{n\geq 0}$. It follows from (30) that the variance of the weighted sum $\{x_n\}_{n\geq 1}$ is $\sigma_x^2 = 1$.

The proposed leak detection method is generic but in the case of a real SFR HE, a calibration phase should be considered. The normal operating noise corresponding to $\mathcal{H}_0$ can be obtained during the first minutes at full power. During this time, the passive acoustic detection is not operational, and hence this period is a natural candidate as a calibration phase. The vibro-acoustic detection can only be used in addition to another detection media (electro chemical hydrogen meter for water or spectral analysis in a pressurized tank for nitrogen) and the other media confirms that there is no leak during recording time. Thanks to this other detection media, it is possible to delicately extend operating conditions or update $\mathcal{H}_0$ by using the recordings done a few minutes (or a long time) earlier.

The alternative hypothesis $\mathcal{H}_1$ (there is a leak) is defined as a weighted sum of normal operating noise defined in (30) and the vibro-acoustic signals coming from the installations IKHAR corresponding to the nitrogen injection (simulation of a leak) under different pressure

$$\mathcal{H}_1 \ : \quad (y_0, \ldots, y_{N-1}) = (x_0, \ldots, x_{N-1}) + \frac{\sqrt{\mathrm{SNR}}}{\sigma_s} (s_0, \ldots, s_{N-1}) , \qquad (31)$$

where $s_0, \ldots, s_{N-1}$ is the vibro-acoustic signal coming from the installation IKHAR with the nitrogen injection, σ_s is the SD of the signal $\{s_n\}_{n\geq 0}$ and SNR is the signal-to-noise ratio. Because the accelerometer position and the vibro-acoustic environment in the real-life situation can be different from the position and environment of mock-ups IKHAR and DIADEMO, the SNR coefficient permits to vary the complexity of the leak detection problem.

In the absence of the theoretical PSD corresponding to normal operating noise and to the signal (a small leak simulated by the nitrogen injection), we have to use the parametric AR model extracted from the data. Following the definition of the null $\mathcal{H}_0$ and alternative $\mathcal{H}_1$ hypotheses (30) – (31), the PSD of

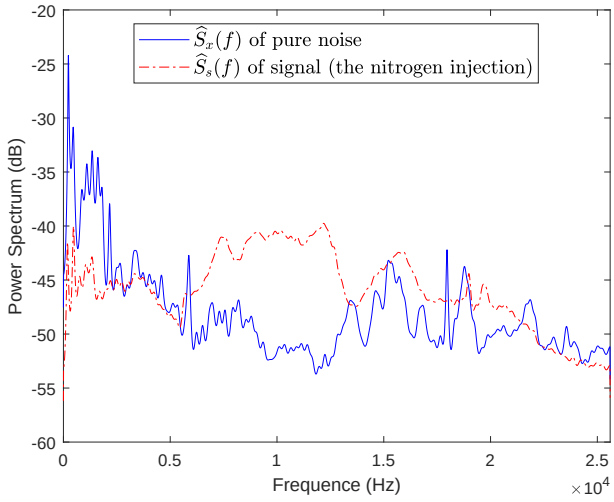

Figure 2: The estimated PSD $\widehat{S}_y(f)$ corresponding to normal operating noise and to the signal (there is a leak in the HE).

$\mathcal{H}_0$ and $\mathcal{H}_1$ hypotheses are given as follows

$$\mathcal{H}_0 \ : S_y(f) = S_x(f) = \widehat{S}_x(f) \text{ against } \mathcal{H}_1 \ : S_y(f) = S_{x+s}(f) = \widehat{S}_x(f) + \frac{\text{SNR}}{\widehat{\sigma}_s^2}\widehat{S}_s(f), \tag{32}$$

where $0 \leq f \leq F_s/2$, $\widehat{S}_x(f)$ is the AR(200) model-based estimated PSD of normal operating noise records simulated by using the mixture (IKHAR and DIADEMO) defined by (30) with the weighted coefficients $w_1 = \sqrt{0.7}$ and $w_2 = \sqrt{0.3}$, $\widehat{\sigma}_x$ is the SD of this mixture, $\widehat{S}_s(f)$ is the AR(200) model-based estimated PSD by using a signal record (IKHAR with the nitrogen injection at 36 bar pressure) and mixed with the PSD of normal operating noise following the SNR, as defined in (31), and $\widehat{\sigma}_s$ is the SD of the recorded signal. The estimated PSD of pure noise $\widehat{S}_x(f)$ and signal $\widehat{S}_s(f)$ are shown in Figure 2. The PSD $S_x(f)$ (resp. $S_{x+s}(f)$) defining the hypothesis $\mathcal{H}_0$ (resp. $\mathcal{H}_1$) are shown in Figure 3 for SNR $= -13$ dB and -23. The PSD $S_{y,1}(f)$ defining the hypothesis $\mathcal{H}_1$ with SNR $= -30$ dB is not shown because the difference between $\mathcal{H}_0$ and $\mathcal{H}_1$ is invisible to the eye for SNR $= -30$ dB.

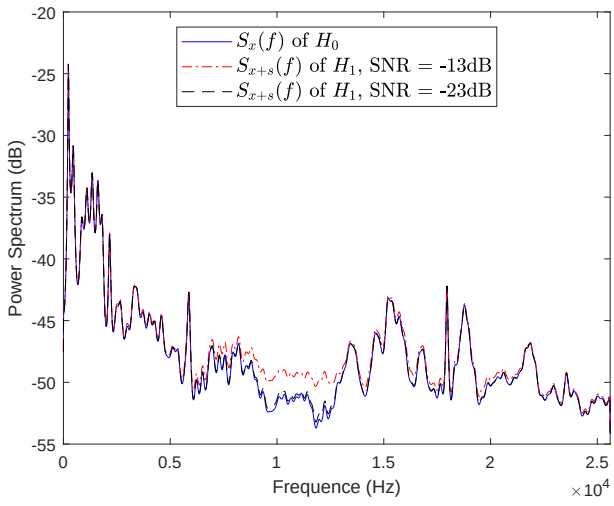

Figure 3: The PSDs $S_x(f)$ and $S_{x+s}(f)$ defining the hypotheses $\mathcal{H}_0$ and $\mathcal{H}_1$ with SNR $= -13$ dB and -23.

5. Results of simulation

This section is devoted to two tasks. The first task is to compute the upper bound $\overline{\alpha}_1$ for the worst-case probability of missed detection $\overline{\mathbb{P}}_{\rm md}(T_{\rm FMA})$ as a function of the upper bound $\overline{\alpha}_0$ for the worst-case probability of false alarm $\overline{\mathbb{P}}_{\rm fa}(T_{\rm FMA}; m_\alpha)$ and to verify the asymptotic equations (26) – (28) by using the Monte-Carlo simulation. The second task is to test the FMA detector by using the records of real signals coming from the installations IKHAR and DIADEMO.

Because the target values of $\overline{\alpha}_0$ and $\overline{\alpha}_1$ are very small, it seems to be unrealistic to estimate the probabilities $\overline{\mathbb{P}}_{\rm md}(T_{\rm FMA})$ and $\overline{\mathbb{P}}_{\rm fa}(T_{\rm FMA}; m_\alpha)$ by using a conventional Monte-Carlo simulation. Instead, a $2 \cdot 10^3$ Monte-Carlo simulation has been performed to estimate the expectation and variance of the LLR given by (24). Next, the bound $\overline{\alpha}_1$ has been calculated as a function of $\overline{\alpha}_0$ by using equation (28) under asymptotic assumption of the LLR Gaussianity. The null hypothesis $\mathcal{H}_0$ is defined by the PSD (32) of normal operating noise simulated by the weighted sum (30) of the IKHAR (without nitrogen injection) and DIADEMO records. The alternative hypothesis $\mathcal{H}_1$ is defined by the PSD

(32) estimated from the weighted sum of three signals. Two first signals are the IKHAR (without nitrogen injection) and DIADEMO. They produce a weighted sum (30), corresponding to the hypothesis $\mathcal{H}_0$. The third signal, simulating the HE leak, is represented by another IKHAR record with the nitrogen injection at 36 bar pressure and it is added to the previous signals with a given SNR (see (31)).

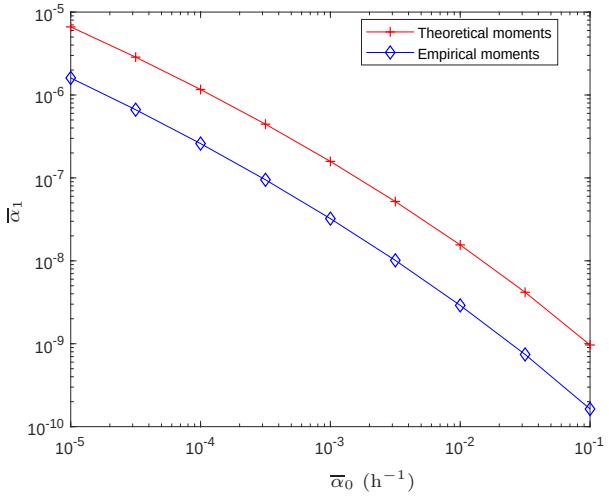

Figure 4: The probability $\overline{\alpha}_1$ as a function of $\overline{\alpha}_0$ for SNR -30 dB calculated by using theoretical moments (26), (27) and empirical moments obtained by a $2 \cdot 10^3$ Monte-Carlo simulation.

The required time-to-alert is 60 sec, $F_s = 51.2$ kHz, $K = 375$, $L = 8192$, $N = KL$, the reference period for false alarm is 3600 sec or 1 h, $m_\alpha = 22500$, $f_{k_1} = 6$ kHz and $f_{k_2} = 13$ kHz. The probability of false alarm is measured per hour (h^{-1}). The results of asymptotic equations and Monte-Carlo simulations for the FMA test provided that SNR $= -30$ dB and SNR $= -33$ dB are shown in Figures 4 and 5. The upper bound $\overline{\alpha}_1$ for the worst-case probability of missed detection $\overline{\mathbb{P}}_{\mathrm{md}}(T_{\mathrm{FMA}})$ as a function of the upper bound $\overline{\alpha}_0$ for the worst-case probability of false alarm $\overline{\mathbb{P}}_{\mathrm{fa}}(T_{\mathrm{FMA}}; m_\alpha)$ calculated by using the asymptotic equation (28) with theoretical moments (26) – (27) of the LLR are shown by solid lines with plus symbols. The same functions calculated with empirical

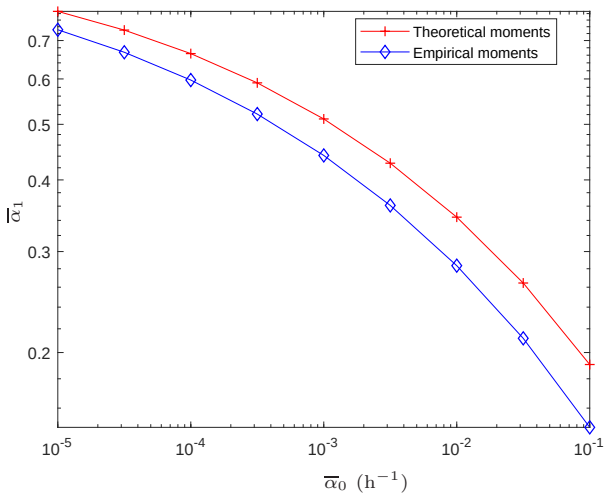

Figure 5: The same functions as in Figure 4 for SNR −33 dB.

moments of the LLR obtained by a $2 \cdot 10^3$ Monte-Carlo simulation are shown by solid lines with diamond symbols.

Let us briefly discuss the results of the comparison between the asymptotic equations and Monte-Carlo simulations. First of all, it is worth noting the existence of some difference observed between the curves representing $\overline{\alpha}_1$ as a function of $\overline{\alpha}_0$ calculated by using the theoretical moments and the same curves calculated by using the empirical moments of the LLR given by equations (26) – (27) (see Figures 4 and 5). The reason for this difference is explained by non-asymptotic properties of the vector $\widehat{S}_y^i(f_{k_1}), \ldots, \widehat{S}_y^i(f_{k_2})$ for $K = 375$ and $L = 8192$. As it follows from [25, Ch 10.3] and [26, Ch 8.2.2], $\widehat{S}_y^i(f_k)$ and $\widehat{S}_y^i(f_\ell)$ with $k \neq \ell$ are independent and exponentially distributed only asymptotically. For finite values of L there are small additional terms to the expectation $\mathbb{E}\left[\widehat{S}_y^i(f_k)\right]$, variance $\mathrm{var}\left[\widehat{S}_y^i(f_k)\right]$ and covariance $\mathrm{cov}\left[\widehat{S}_y^i(f_k), \widehat{S}_y^i(f_\ell)\right]$ with $k \neq \ell$. These additional terms cannot be easily estimated but they lead to additional biases in the empirical moments (26) – (27) of the LLR. Finally, the theoretical moments lead to some overestimation of $\overline{\alpha}_1$ as a function of $\overline{\alpha}_0$ (see the solid lines with plus symbols in Figures 4 and 5).

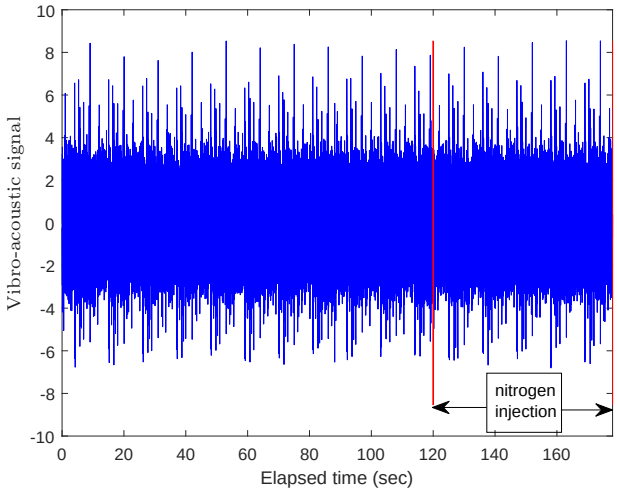

Figure 6: The mixture of the IKHAR and DIADEMO records following (30) – (31). The leak of the HE is simulated by the nitrogen injection at 36 bar pressure starting from $t_0 = 120$ sec. The SNR is -23 dB.

Second, the very weak signals (with SNR $= -30$ dB) of the nitrogen injection at 36 bar pressure can be detected with low probabilities of missed detection $\overline{\mathbb{P}}_{\rm md}(T_{\rm FMA}) \leq \overline{\alpha}_1 \leq 10^{-5}$ and false alarm $\overline{\mathbb{P}}_{\rm fa}(T_{\rm FMA}; m_\alpha) \leq \overline{\alpha}_0 \leq 10^{-5}{\rm h}^{-1}$. But if the SNR will be even more reduced from -30 dB to -33 dB, then the missed detection probability drastically increases to an unacceptable level, i.e., $\overline{\mathbb{P}}_{\rm md}(T_{\rm FMA}) \leq \overline{\alpha}_1 \in [0.2, 0.7]$ for $\overline{\mathbb{P}}_{\rm fa}(T_{\rm FMA}; m_\alpha) \leq \overline{\alpha}_0 \in [10^{-5}, 10^{-1}]{\rm h}^{-1}$. Hence, SNR $= -30$ dB represents a minimal SNR value detectable with acceptable probabilities $\overline{\mathbb{P}}_{\rm md}(T_{\rm FMA})$ and $\overline{\mathbb{P}}_{\rm fa}(T_{\rm FMA}; m_\alpha)$ by using the proposed FMA detector.

Let us discuss the test of the FMA detector by using the real data coming from the mock-ups IKHAR and DIADEMO. The length of the IKHAR record is not large enough to cover the records DIADEMO. For this reason, the IKHAR record has been repeated each 11 sec to prepare the mixture of the IKHAR and DIADEMO records. As previously, for tuning the FMA test, the null hypothesis $\mathcal{H}_0$ (normal operating noise) is defined by the PSD estimated from the weighted sum of the IKHAR (without nitrogen injection) and DIADEMO

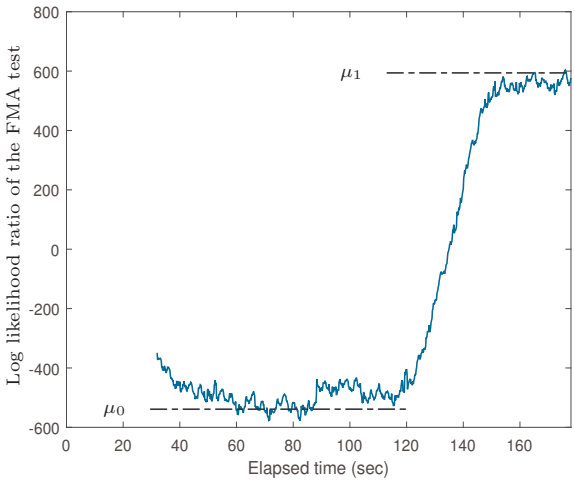

Figure 7: The LLR of FMA test as a function of elapsed time.

record and the alternative hypothesis $\mathcal{H}_1$ is defined by the PSD estimated from the weighted sum of pure noise and the signal represented by the IKHAR record corresponding to the nitrogen injection at 36 bar pressure. In both cases, the duration of records used for tuning is 11 sec. The required time-to-alert now is 32 sec, $F_s = 51.2$ kHz, $K = 200$, $L = 8192$, $N = KL$, $f_{k_1} = 9.5$ kHz and $f_{k_2} = 12.5$ kHz.

The results of real data processing are shown in Figures 6 and 7. The change-point or the instant of nitrogen injection (simulation of a leak) is $t_0 = 120$ sec (shown by the solid red vertical line in Figure 6). The SNR is equal to -23 dB. The picture on the left attests that the presence of the vibro-acoustic signal simulating a leak is invisible to the eye. The picture on the right shows that the total LLR begins to grow from $t_0 = 120$ sec to $t = 152$ sec. After this time, the LLR remains stable. The theoretical values μ_0 and μ_1 of the total LLR expectation obtained by tuning on 11 sec duration records are shown by two horizontal dash-dotted lines. It can be concluded that the total LLR values Λ_{m-K+1}^{m}, $m \geq K$, are in concordance with the asymptotic LLR expectations

μ_0 and μ_1 before the instant $t_0 = 120$ sec and after the instant $t = 152$ sec. Some deviations from the asymptotic LLR expectations are explained by the non-stationarity of the processed signals.

6. Discussion of some possible extensions

The solution to the problem of the HE leak detection proposed in Section 3 and examined in Section 5 is based on the assumption that the PSD of normal operating noise $f \mapsto S_x(f)$ and the PSD of the additive sum of normal operating noise and the signal due to a leak $f \mapsto S_{x+s}(f)$ are perfectly known and constant. These working hypotheses correspond to the main goal of this paper to check the feasibility of the proposed leak detection algorithm. Nevertheless, the application of this technique to the vibro-acoustic signals coming from a real HE necessitates some potential extension of such working hypotheses.

First of all, let us discuss the reliable leak detection during the transition from one normal operating condition of the HE to another one. As it follows from the FMA detector definition (23) – (25) and its flowchart shown in Figure 1, the detector is uniquely defined by the PSDs $f \mapsto S_x(f)$ and $f \mapsto S_{x+s}(f)$ of the pre-change and post-change signals. Hence, if the leak detection system is equipped with a mechanism of adaptation to the current normal operating noise PSD, the FMA detector reloads the current PSDs $f \mapsto S_x(f)$ and $f \mapsto S_{x+s}(f)$ at each step m of leak detection (see the flowchart shown in Figure 1). It is worth noting that some *a priori* information about the shape of the signal PSD $f \mapsto S_s(f)$ corresponding to a small leak in the HE and the minimum required SNR should be available to calculate $f \mapsto S_{x+s}(f)$ in the real time. The idea to associate a change detection algorithm to an adaptive estimation algorithm has been initially considered in [49, 50]. For the time-variant (non-stationary) system, it is necessary to have a prior model of system dynamics to design an optimal estimation algorithm. In the case when such *a priori* information is absent, the tracking properties of the adaptive RLS estimator of AR model and its PSD is defined by a single tuning parameter, i.e., the forgetting factor

$0 < \lambda < 1$ (for details see [48, 50, 27]).

Second, let us discuss an extension of the proposed FMA detector to the case of the gradual spectral changes developing in time. In other words, the generative model of segments (7) is re-written as follows :

$$\widehat{S}_y^i(f_k) \sim \begin{cases} \mathrm{Exp}\left(S_x(f_k)\right) & \text{if} \quad i < i_0, \\ \mathrm{Exp}\left(S_{x+s}^{i-i_0+1}(f_k)\right) & \text{if} \quad i \geq i_0 \end{cases} \quad \text{for } f_k = \frac{k}{L}F_s \text{ and } k = k_1, \ldots, k_2, \tag{33}$$

where $0 \leq k_1 \leq k_2 \leq L/2$. Therefore, the detection of gradual spectral changes is reduced to the sequential detection of gradual changes in the distribution of the vector of peridodogram $\left(\widehat{S}_y^i(f_{k_1}) \ldots, \widehat{S}_y^i(f_{k_2})\right)$ of the observed sequence of segments. These gradual changes are defined by the profiles $S_{x+s}^1(f_k), \ldots, S_{x+s}^K(f_k)$ for each frequency f_k, where K is the required number of segments to alert.

Let us adopte the LLR (23) to the case of gradual changes. The LLR between the hypotheses $\mathcal{H}_0$ and $\mathcal{H}_1^{i-i_0+1}$ for the frequency f_k is written for the i-th segment as follows

$$\Lambda_i(f_k) = \log \frac{S_x(f_k)}{S_{x+s}^{i-i_0+1}(f_k)} + \left[\frac{1}{S_x(f_k)} - \frac{1}{S_{x+s}^{i-i_0+1}(f_k)}\right] \widehat{S}_y^i(f_k) \quad \text{for } i \geq i_0, \tag{34}$$

The LLR in the moving window of K segments $Y_{m-K+1}, \ldots, Y_m$ is given by :

$$\Lambda_{m-K+1}^m(f_k) = \sum_{i=m-K+1}^{m} \log \frac{S_x(f_k)}{S_{x+s}^{i+K-m}(f_k)} + \left[\frac{1}{S_x(f_k)} - \frac{1}{S_{x+s}^{i+K-m}(f_k)}\right] \widehat{S}_y^i(f_k), \tag{35}$$

where i is the number of segment of size L, $\widehat{S}_y^i(f_k)$ is the periodogram corresponding to the frequency f_k and calculated for the i-th segment Y_i. Therefore, the total LLR for all the frequencies $f_{k_1}, \ldots, f_{k_2}$ is obtained by summation equation (35) and the FMA stopping rule is given as follows

$$T_{\mathrm{FMA}} = \inf\left\{m \geq K : \Lambda_{m-K+1}^m \geq h\right\}, \quad \Lambda_{m-K+1}^m = \sum_{k=k_1}^{k_2} \Lambda_{m-K+1}^m(f_k). \tag{36}$$

Finally, let us briefly discuss how the proposed HE leak detection algorithm can be coupled with other algorithms predicting the accidents such as LOCA

[3, 4]. As it is advocated in [3], the early and reliable detection of even a small HE leak is an important task for the subsequent successful processing of such an accident. On the other hand, a method of the leak rate prediction before break (in the framework of the LBB concept) by using two types of the artificial neural network (ANN): three-layer back propagation network (BPN) and genetic neural network (GNN) has been considered in [4]. By using these ANNs, a model is designed to explain the output parameter (Reynolds number) with the aid of six dimensionless inputs by minimizing the quadratic criterion. These inputs are the thermodynamic properties and crack morphologies. The proposed HE leak detection algorithm can be coupled to the LBB leakage prediction as a kind of trigger. Such a trigger will switch the nominal regime mode of a periodic application of the ANN-based LBB leakage prediction to a reinforced regime when the risk of break becomes too important and, hence, the application of the ANN-based LBB leakage prediction should be very frequent.

7. Conclusion

The detection of leaks in a prototype of a sodium-gas SFR HE has been considered in the paper. The HE should be permanently monitored in order to detect a leak of nitrogen into the sodium circuit, which can affect the SFR performance or safety. The records coming from two experimental mock-ups installed at CEA/Cadarache for simulating normal operating noise and abnormal noise (with leaks) have been used to assess the proposed solution.

The significance of this research with respect to the previously published works is twofold. First, the proposed solution allows reliable detection of a small leak with the minimal SNR of -30 dB provided that the detection delay, the missed detection probability and the false alarm probability are respected, which is much better than the usually requested SNR of -17 dB. Second, an analytical method for calculation of the probabilities of missed detection and the false alarm has been proposed. This method guarantees the required statistical properties of the proposed test. The following detailed conclusions can be drawn.

1. The spectral analysis of the records coming from two mock-ups at CEA/Cadarache permits to establish the descriptions of the null hypothesis $\mathcal{H}_0$ (normal operating noise coming from the HE and other equipment like pumps, turbine, etc.) and alternative hypothesis $\mathcal{H}_1$ (an additive sum of normal operating noise and the useful signal corresponding to a leak of the HE).
2. The proposed leak detection solution is based on the adaptation of the FMA test applied to the periodogram to reliably detect an abrupt change in the spectral density of measured signals.
3. Asymptotic equations for the calculation of the relation between the upper bound $\overline{\alpha}_1$ for the worst-case probability of missed detection $\overline{\mathbb{P}}_{\mathrm{md}}(T_{\mathrm{FMA}})$ and the upper bound $\overline{\alpha}_0$ for the worst-case probability of false alarm $\overline{\mathbb{P}}_{\mathrm{fa}}(T_{\mathrm{FMA}}; m_\alpha)$ during the reference period m_α have been proposed. These equations can be used as a preliminary approximate method to quantitatively predict the statistical properties of the FMA test.
4. Without taking into account the impact of signal non-stationarity under the null hypothesis $\mathcal{H}_0$, the FMA test is able to detect a leak in the HE with SNR ≥ -30 dB with low probabilities of false alarm $\overline{\mathbb{P}}_{\mathrm{fa}}(T_{\mathrm{FMA}}; m_\alpha) \leq \overline{\alpha}_0 \leq 10^{-5}\mathrm{h}^{-1}$ and missed detection $\overline{\mathbb{P}}_{\mathrm{md}}(T_{\mathrm{FMA}}) \leq \overline{\alpha}_1 \leq 10^{-5}$ provided that the detection delay is upper bounded by 60 sec. It is worth noting that $10^{-5}\mathrm{h}^{-1}$ corresponds to the level "one false alarm per 11 years". In these basic conditions, the FMA test detection capability is much better than the usually requested SNR of -17 dB, which is expected for 1 g/sec leaks, see [21].
5. The impact of non-stationarity on the minimal detectable SNR and the precision/applicability of asymptotic equations for $\overline{\alpha}_0$ and $\overline{\alpha}_1$ will be examined in a future study.
6. Testing the detection performance of the FMA test coupled with the periodogram by using the real data coming from the mock-ups simulating the sodium-water HE will be considered in a future study.

In parallel to the improvement of the detection methods, the obtaining of leak detector performances in fully representative SFR HE leak conditions is a topic for consideration.

ACKNOWLEDGMENTS

The authors gratefully acknowledge the research and financial support of this work from the Commissariat à l'Energie Atomique et aux Energies Alternatives, France. The authors would like to thank the anonymous reviewers for their detailed comments, which improved the paper.

References

[1] J. Ph. Jeannot, T. Gnanasekaran, C. Latge, R. Sridharan, L. Martin, R. Ganesan, J. Augem, J. Courouau, G. Gobillot (2009) In-sodium hydrogen detection in the Phenix fast reactor steam generator: a comparison between two detection methods, In the Proceedings of the 1st International Conference on Advancements in Nuclear Instrumentation, Measurement Methods and their Applications, Marseille, France.

[2] N. Matta, Y. Vandenboomgaerde, J. Arlat (Eds.) (2012) Supervision and Safety of Complex Systems. ISTE, Wiley

[3] R. K. Singh and A. R. Rao (2011) Steam leak detection in advance reactors via acoustics method, *Nuclear Engineering and Design*, 241(7), 2448–2454

[4] Zhang, J., Chen, R.H., Wang, M.J., Tian, W.X., Su, G.H., and Qiu, S.Z. (2017) Prediction of LBB leakage for various conditions by genetic neural network and genetic algorithms, *Nuclear Engineering and Design*, vol. 325, pp. 33-43.

[5] A. R. Marklund, F. Michel (2015) Application of a new passive acoustic leak detection approach to recordings from the Dounreay prototype fast reactor. *Annals of Nuclear Energy*, 85, 175–182

[6] A. R. Marklund, S. Kishore, V. Prakash, K. K. Rajan, F. Michel (2016) Passive acoustic leak detection for sodium cooled fast reactors using hidden Markov models. *IEEE Transactions on Nuclear Science* , 63(3), June 2016, 1463 - 1470.

[7] Voss, J., and Arnaoutis, N. (1984). Recent experiments on acoustic leak detection. International Atomic Energy Agency, Vienna (Austria). International Working Group on Fast Reactors; 180 p; Dec 1984; p. 95-101

[8] Greene, D. A., Malovrh, J. W., Gaubatz, D. C., and Calkins, C. A. (1985). GAAD system demonstration of rapid acoustic detection of simulated intermediate water leak in prototype steam generator. (No. GEFR-00718), General Electric Co., Sunnyvale, CA (United States). Advanced Nuclear Technology Operation.

[9] Kassab, S., Michel, F., Maxit, L. (2019) Water experiment for assessing vibroacoustic beamforming gain for acoustic leak detection in a sodium-heated steam generator. *Mechanical Systems and Signal Processing*, Elsevier, vol. 134, pp. 106332.

[10] Chikazawa, Y., Yoshiuji, T. (2015) Water experiment on phased array acoustic leak detection system for sodium-heated steam generator, *Nuclear Engineering and Design*, Elsevier, vol. 289, pp. 1-7,

[11] M.S. Chenaud, N. Devictor, G. Mignot, F. Varaine, C. Vénard, L. Martin, M. Phelip, D. Lorenzo, F. Serre, F. Bertrand, N. Alpy, M. Le Flem, P. Gavoille, R. Lavastre, P. Richard, D. Verrier, D. Schmit (2013) Status of the ASTRID core at the end of the pre-conceptual design phase 1, *Nuclear Engineering and Technology*, 45(6), 721–730

[12] A. R. Marklund, F. Michel, H. Anglart (2017) Demonstration of an improved passive acoustic fault detection method on recordings from the Phénix steam generator operating at full power. *Annals of Nuclear Energy*, 101, 1–14

[13] Bakhache, B. and Nikiforov, I. (2000). Reliable detection of faults in measurement systems. *International Journal of Adaptive Control and Signal Processing*, 14(7), 683–700.

[14] Guepie, B., Fillatre, L. and Nikiforov, I. (2012). Sequential Monitoring of Water Distribution Network. In the Proceeding of the SYSID 2012, 16th IFAC Symposium on System Identification, Brussels, Belgium, July 11-13.

[15] Guépié B. K., Fillatre L., and Nikiforov, I. (2012). Sequential detection of transient changes. *Sequential Analysis*, vol. 31, no. 4, pp. 528–547.

[16] Guépié, B. K., Fillatre, L. and Nikiforov, I. (2017) Detecting a suddenly arriving dynamic profile of finite duration. *IEEE Trans. on Information Theory*, vol. 63(5), 3039 – 3052.

[17] Srinivasan, G. S., Singh, O. P. and Prabhakar, R. (2000). Leak noise detection and characterisation using statistical features. Annals of Nuclear Energy, 27(4), 329–343.

[18] Kalyanasundaram, P., Raj, B., Prakash, V. and Ranga, R. (2013). Detection of Simulated Steam Leak into Sodium in Steam Generator of PFBR by Argon Injection Using Signal Analysis Techniques. Nuclear Technology, 182(3), 249–258.

[19] Liu, Z. H., Niu, X. D., Mu, G. Y., Wang, X., Zhang, H. and Pang, Y. J. (2005). Method for acoustic leak detection of fast reactor steam generator using maximum modulus based on wavelet transform. In 2005 International Conference on Machine Learning and Cybernetics (Vol. 2, pp. 737–741), August, IEEE.

[20] Riber Marklund, A. (2016). Passive acoustic leak detection in energy conversion systems of sodium fast reactors. Doctoral Dissertation, Nuclear Reactor Technology, Department of Physics, KTH Royal Institute of Technology, Sweden

[21] IAEA-TECDOC-946 (1997). Acoustic signal processing for the detection of sodium boiling or sodium-water reaction in LMFRs, Report of the International Atomic Energy Agency, IAEA, Vienna, May, 254 p.

[22] Kim, T. J., Yugay, V. S., Jeong, J.-Y., Kim, J.-M., Kim, B.-H., Lee, T.-H., Lee Y.-B., Kim Y.-I. and Hahn, D. (2010). Acoustic leak detection technology for water/steam small leaks and microleaks into sodium to protect an SFR steam generator. Nuclear Technology, 170(2), 360–369.

[23] Box, G., and Jenkins, G. (1976) *Time Series Analysis : Forecasting and Control*. Holden-Bay, San Francisco.

[24] Brillinger, D.R. (1981) *Time Series, Data Analysis and Theory*. Rinehart & Winston, New-York.

[25] Brockwell, P.J. and Davis, R.A. (1987) *Time Series: Theory and Methods*. Springer-Verlag, New-York Inc.

[26] Hayes, M. H. (1996) *Statistical Digital Signal Processing and Modeling*. New York: Wiley.

[27] Manolakis, D. G. and Ingle, V. K. and Kogon S. M. (2005) *Statistical and Adaptive Signal Processing*. Artech House.

[28] Chikazawa, Y. and Yoshiuji, T. (2015). Water experiment on phased array acoustic leak detection system for sodium-heated steam generator. Nuclear Engineering and Design, 289, pp. 1–7.

[29] Basseville, M. and Nikiforov, I.V. (1993). *Detection of Abrupt Changes: Theory and Application*. Prentice Hall. [Online]. Available: `http://www.irisa.fr/sisthem/kniga`.

[30] Lai, T.L. (2001). Sequential analysis : some classical problems and new challenges (with discussion). *Statistica Sinica*, 11, 303–408.

[31] Poor, H. V. and Hadjiliadis, O. (2009). *Quickest detection*. Cambridge University Press.

[32] A. Tartakovsky, I. Nikiforov, and M. Basseville, *Sequential Analysis : Hypothesis Testing and Changepoint Detection*. CRC Press, Taylor & Francis Group, 2014.

[33] Shiryaev, A.N. (1961). The detection of spontaneous effects. *Soviet Mathematics – Doklady*, 2, 740–743. Translation from Doklady Akademii Nauk SSSR, 138 : 799–801, 1961.

[34] Shiryaev, A.N. (1963). On optimum methods in quickest detection problems. *Theory of Probability and its Applications*, 8(1), 22–46.

[35] Lorden, G. (1971). Procedures for reacting to a change in distribution. *The Annals of Mathematical Statistics*, 42(6), 1897–1908.

[36] Page, E.S. (1954). Continuous inspection schemes. *Biometrika*, 41(1-2), 100–114.

[37] Moustakides, G. (1986). Optimal stopping times for detecting changes in distribution. *Annals of Statistics*, 14(4), 1379–1387.

[38] Bansal, R.K. and Papantoni-Kazakos, P. (1986). An algorithm for detecting a change in a stochastic process. *IEEE Trans. on Information Theory*, 32(2), 227–235.

[39] Lai, T.L. (1995). Sequential changepoint detection in quality control and dynamical systems. *Jal Royal Statistical Society B*, 57(4), 613–658.

[40] Lai, T.L. (1998). Information bounds and quick detection of parameter changes in stochastic systems. *IEEE Trans. on Information Theory*, 44(7), 2917–2929.

[41] A. Wald, (1947). *Sequential Analysis*, ser. Dover Phoenix Editions. Dover Publications, 2004. [Online]. Available: `http://books.google.fr/books?id=oVYDHHzZtdIC`

[42] C. Han, P. K. Willett, B. Chen, and D. A. Abraham, "A detection optimal min-max test for transient signals," *IEEE Trans. on Information Theory*, vol. 44, no. 2, pp. 866–869, Mar. 1998.

[43] R. Streit and P. Willett, "Detection of random transient signals via hyperparameter estimation," *IEEE Trans. Signal Process.*, vol. 47, no. 7, pp. 1823–1834, Jul. 1999.

[44] C. Han, P. Willett, and D. Abraham, "Some methods to evaluate the performance of Page's test as used to detect transient signals," *IEEE Trans. Signal Process.*, vol. 47, no. 8, pp. 2112–2127, Aug. 1999.

[45] B. Chen and P. Willett, "Detection of hidden Markov model transient signals," *IEEE Trans. Aerosp. Electron. Syst.*, vol. 36, no. 4, pp. 1253–1268, 2000.

[46] Z. Wang and P. Willett, "A performance study of some transient detectors," *IEEE Trans. Signal Process.*, vol. 48, no. 9, pp. 2682–2685, Sep. 2000.

[47] Z. J. Wang and P. Willett, "A variable threshold Page procedure for detection of transient signals," *IEEE Trans. Signal Process.*, vol. 53, no. 11, pp. 4397–4402, 2005.

[48] Ljung, L., and Söderström, T. (1985) *Theory and practice of recursive identification.* MIT Press series in signal processing, optimization, and control, 529 p.

[49] Benveniste, A., Basseville M., and Moustakides, G. (1987) The asymptotic local approach to change detection and model validation. *IEEE Transactions on Automatic Control*, vol. 32, no. 7, pp. 583–592, July.

[50] Gustafsson, F. (2000) *Adaptive Filtering and Change Detection.* John Wiley & Sons, Ltd, 500 p.